Published in final edited form as:
Cancer Res. 2009 March 1; 69(5): 2133–2140. doi:10.1158/0008-5472.CAN-08-1405.

GM-CSF INHIBITS BREAST CANCER GROWTH AND METASTASIS BY INVOKING AN ANTI-ANGIOGENIC PROGRAM IN TUMOR-EDUCATED MACROPHAGES

Tim D. Eubank[2,*], **Ryan D. Roberts**[1,*], **Mahmood Khan**[3], **Jennifer M. Curry**[1], **Gerard J. Nuovo**[4], **Periannan Kuppusamy**[3], and **Clay B. Marsh**[2]

[1]Integrated Biomedical Science Graduate Program, College of Medicine and Public Health, The Dorothy M. Davis Heart and Lung Research Institute, The Ohio State University, Columbus, OH 43210, USA

[2]Division of Pulmonary, Allergy, Critical Care, and Sleep Medicine, Department of Internal Medicine, The Dorothy M. Davis Heart and Lung Research Institute, The Ohio State University, Columbus, OH 43210, USA

[3]Davis Heart and Lung research Institute, Division of Cardiovascular Medicine, Department of Internal Medicine, The Dorothy M. Davis Heart and Lung Research Institute, The Ohio State University, Columbus, OH 43210, USA

[4]Comprehensive Cancer Center, Department of Pathology, The Dorothy M. Davis Heart and Lung Research Institute, The Ohio State University, Columbus, OH 43210, USA

Abstract

Tumor-educated macrophages facilitate tumor metastasis and angiogenesis. We discovered that GM-CSF blocked macrophages VEGF activity by producing soluble VEGF receptor-1 (sVEGFR-1) and determined the effect on tumor-associated macrophage behavior and tumor growth. We show GM-CSF treatment of murine mammary tumors slowed tumor growth and slowed metastasis. These tumors had more macrophages, fewer blood vessels, and lower oxygen concentrations. This effect was sVEGFR-1 dependent. *In situ* hybridization and flow cytometry identified macrophages as the primary source of sVEGFR-1. These data suggest that GM-CSF can re-educate macrophages to reduce angiogenesis and metastases in murine breast cancer.

INTRODUCTION

Cells in the tumor environment facilitate tumor growth and spread. Tumor cells influence endothelial cells, macrophages, T cells, and fibroblasts to evade host defenses, undergo angiogenesis, and produce factors that promote growth, survival, and metastases[1].

Tumors grow through signals elicited from cells in their microenvironment. For instance, some tumors downregulate immune surveillance molecules to avoid attack by T-cells and NK cells[2, 3]. Some secrete growth factors that stimulate blood vessel formation[4]. Other tumors stop making molecules that maintain cell-cell interactions[5]. Changes tumors impose on

Clay B. Marsh, MD, Clay.Marsh@osumc.edu, 614-293-9309, Fax: 614-688-4662.
*These authors contributed equally.

Disclosure: The authors of this study declare that they have no competing interests with the data presented in this paper

surrounding cells are called "tumor education"[6], and often represent an inappropriate triggering of developmental programs within the tumor cells[7].

One type of immune cell, the macrophage, plays an important role in normal breast tissue development. Macrophage activity, stimulated by macrophage colony-stimulating factor (M-CSF), is essential for normal breast development[8]. In breast tumors, macrophages constitute up to 35% of the infiltrating inflammatory cells[9]. These tumor-associated macrophages (TAMs) produce factors that facilitate tumor invasion and angiogenesis, such as MMPs[10] and VEGF[11].

The cytokine milieu in the tumor microenvironment dictates macrophage behavior. Many breast tumors secrete M-CSF, which is expressed in over 70% of human breast cancers[12]. Serum M-CSF levels correlate with tumor size, metastasis, and poor outcomes in humans[13, 14]. Mice deficient in M-CSF are protected against breast tumor metastasis, and re-expressing M-CSF solely in the breast tissue restores metastatic activity[15]. This effect likely involves both an M-CSF/EGF paracrine loop between tumors and macrophages[16] and M-CSF-induced VEGF production[11], inducing angiogenesis[17].

In sharp contrast, GM-CSF-stimulated monocytes exhibit anti-tumor behavior. GM-CSF enhances macrophage antigen presentation and immune responsiveness[18]. We showed that GM-CSF stimulates monocytes to secrete sVEGFR-1, which binds and inactivates VEGF and blocks angiogenesis[19]. Angiogenesis within the tumors is necessary for tumor progression, as tumors cannot grow beyond a few cubic millimeters without blood vessel formation to supply oxygen and nutrients.[20, 21].

Recent studies illustrate the importance of sVEGFR-1 in blocking cancer progression. For example, low intra-tumor sVEGFR-1 and high total VEGF are associated with poor disease-free and overall survival[22]. Toi et al found that tumors with 10-fold more sVEGFR-1 than VEGF have a favorable prognosis[23]. Other studies show similar findings for patients with colorectal cancer[24], glioblastoma[25], and acute myeloid leukemia[26].

These observations led us to speculate that macrophage behavior was manipulated *in vivo* by GM-CSF. We wanted to know whether the TAM phenotype was reversed by GM-CSF within the tumor microenvironment. We show that intra-tumor GM-CSF injections reversed some of the effects of tumor education and induced an anti-tumor phenotype in tumor-associated macrophages.

MATERIALS AND METHODS

MICE

PyMT transgenic mice were purchased from Jackson Laboratories (Bar Harbor, ME). Mammary tumors from PyMT transgenics were removed and orthotopically injected into normal FVB female mice for these studies.

TUMOR INJECTIONS

MET-1 tumor cells were cultured in DMEM containing 10% FBS, 10 μg/ml insulin, and 5 ng/ml rhEGF. These cells were resuspended in DMEM media at 500,000 cells/100 μl. The cells were orthotopically injected into the number four mammary fat pads of normal female FVB mice (allografts).

TREATMENT STUDY

After tumors became palpable, mice were randomized to treatment groups. PBS or 100 ng rmGM-CSF in 50 μls was administered directly into the tumor. For longer timepoint studies, mice were treated until their tumors reached 2 cm in diameter. For short timepoint studies, seven treatments were administered (three times per week). Tumor dimensions and mouse weight were measured weekly for long timepoint studies or at each treatment for shorter studies. For studies analyzing the effect of neutralizing sVEGFR-1 in combination with GM-CSF treatment, tumors were orthotopically injected. Either PBS, 100 ng rmGM-CSF, 100 ng rmGM-CSF + 4 μg anti-VEGF receptor-1 neutralizing antibody (R&D Systems, AF471), 100 ng rmGM-CSF + 4 μg isotype IgG control (goat), or 4 μg anti-VEGF receptor-1 neutralizing antibody alone in 50 μl was injected directly into the tumors.

EPR OXIMETRY

Lithium octa-n-butoxy 2,3-naphthalocyanine (LiNc-BuO) microcrystals were a gift from Dr. Periannan Kuppusamy, The Ohio State University. 10 mg microcrystals were resuspended in 500 μl DMEM. 25 μl of this suspension was added to 5×10^5 PyMT cells for each 100 μl injection. Oxygen measurements were performed immediately, weekly, and upon sacrifice using *in vivo* EPR oximetry. Measurements of tumor oxygenation were performed using an L-band *in vivo* EPR spectrometer (L-band, Magnettech, Germany). Mice were placed in a right, lateral position with their tumor close to the surface coil resonator. EPR spectra were acquired as single 30-second scans. The instrument settings were: incident microwave power, 4 mW; modulation amplitude, 180 mG; modulation frequency 100 kHz; receiver time constant, 0.2 s. The peak-to-peak width of the EPR spectrum was used to calculate pO2 using a standard calibration curve. Three-dimensional imaging was performed as described previously[27].

EVALUATION OF ANGIOGENESIS

Texas red–conjugated dextran (mol wt 70,000; Molecular Probes, Eugene, OR) was prepared to 6.2 mg/ml in PBS and injected via the tail vein at 20 μg/g of mouse body weight. The mice were sacrificed 5 minutes after administration. Tumor sections were analyzed blindly for fluorescence using a confocal microscope with a 10x objective lens and image insets with a 5x zoom. Functional blood vessels (Texas red-dextran positive) were identified and quantified using Adobe Photoshop CS2.

EVALUATION OF NECROSIS

Necrotic tissue within the tumors of mice was evaluated as described (Achilles, E. G. et al., 2001). Necrosis was quantified in a blinded manner using histogram analysis in Adobe Photoshop CS2 software for the presence of green pixels.

TUMOR METASTASES

The lungs from mice implanted with tumor cells and treated with GM-CSF or PBS were removed, insufflated, fixed in formalin, and stained with hematoxylin. Tumor cell metastases were evaluated by subjecting the lungs to Bright Field light under a stereomicroscope. Each tumor incident was counted in a blinded manner.

IN SITU HYBRIDIZATION

Our protocol for detection of RNAs by *in situ* hybridization has been previously published[28].

IMMUNOHISTOCHEMISTRY

To identify cells producing VEGF or sVEGFR-1 mRNA, serial sections of the tumors were cut and stained for F4/80+ cells. Our immunohistochemical detection protocol is

published[28]. For identification of cell infiltrates in response to treatment, mammary tumors were stained to identify F4/80+ (macrophages) and 7/4 (neutrophils) as well as hematoxylin & eosin (H&E). Total cell influx was analyzed by digital images of the entire tumors and quantified using histogram analysis in Adobe Photoshop CS2 software for brown pixels.

IMMUNOFLUORESCENCE

Macrophage phenotype was determined on tumor sections stained. With primary antibodies: goat anti-mouse arginase I (Santa Cruz, sc-18351) and rabbit anti-mouse iNOS (Abcam, ab15323), at 1:200 dilutions. Secondary antibodies used were chicken anti-goat-Alexa 488 and chicken anti-rabbit-Alexa 594 (Invitrogen). Adjacent tissue sections were processed with primary antibodies omitted (secondaries only). Images were captured on a Zeiss confocal microscope using a 63x objective lens.

FLOW CYTOMETRY

PyMT+ FVB female mice with palpable tumors had injections of PBS or GM-CSF into mammary pad number 4 or 9. After 4 weeks, mice were euthanized and their tumors were removed. Immune cells were separated from tumor by centrifugation over a ficoll density gradient. The buffy layer was removed and resuspended in cold FACS buffer. One half of the cells was incubated 5 minutes on ice with rat IgG, and then stained with PE anti-mouse FLT-1 or isotype. The other half was permeabilized with the BD Cytofix/Cytoperm kit, incubated 5 minutes with rat IgG, then stained with the same antibodies. Both sets of samples were fixed with 4% paraformaldehyde, then run on a BD FACScalibur flow cytometer. Analysis was performed using DeNovo FCS Express v3.

TUMOR ECF ANALYSES

Snap-frozen tumor samples from mice treated with PBS (9 samples) or GM-CSF (14 samples) were crushed into fragments <2 mm in diameter and resuspended with 1:2 weight:volume of 2X PBS and rotated at 4°C for 2 hours. The samples were vortexed then spun for 3 minutes at 5000 RPM. The fluid was subjected to cytokine analysis using the Bio-Rad Bioplex for IL-4, IL-10, M-CSF, and VEGF.

STATISTICAL ANALYSES

For data comparing single independent measurements between two treatment groups, Mann-Whitney U test was used to determine whether observations could have come from identical distributions (metastases, tissue necrosis, immunohistochemical stains). The similar nonparametric Kruskal-Wallis test was used when comparing more than two groups (Texas Red angiogenesis data). When groups were larger and distributions approximated the normal distribution, equality of means between groups was compared by Student's T test. Growth data and ongoing oximetry data were compared by repeated measures ANOVA with Tukey posthoc testing, since measures of an individual mouse from one observation to the next were not independent. Kaplan-Meier survival analyses used Mantel-Cox Log Rank testing to determine differences between groups.

RESULTS

LOCAL TREATMENT WITH GM-CSF SLOWS TUMOR GROWTH IN A MOUSE MODEL OF BREAST CANCER

Based on our previous work[19], we predicted treating tumors locally with GM-CSF would stimulate TAMs to secrete sVEGFR-1, countering tumor-derived VEGF, and blocking angiogenesis[29]. To test this hypothesis, we orthotopically injected MET-1 tumor cells (derived from a PyMT+ FVB mouse) to a single mammary gland of an FVB recipient. We chose to use

the PyMT model because 1) tumor progression in this well-characterized model resembles that seen in human tumors[30], 2) these tumors readily metastasize, and 3) the orthotopic allograft injection model maintains a fully-functional immune system in these mice. Further, we could isolate the tumor site, minimizing problems associated with tumors arising in ten separate mammary pads. When tumors became palpable, we randomized the mice into groups. Mice received intra-tumor injections of equal volumes of PBS or rmGM-CSF three times per week for three weeks. Once a week, tumor measurements were recorded.

Mice treated with GM-CSF demonstrated a 66% reduction in tumor size after three weeks ($p=0.025$, Figure 1A). We let tumors grow until they reached 2 cm in their greatest dimension, at which time the mice were euthanized. Figure 1B demonstrates a three-week increase in median survival (defined as time to 2 cm tumor diameter) of mice treated with GM-CSF (3 weeks vs. 6 weeks, $p=0.010$). GM-CSF-treated mice had no significant changes in body weight or overt clinical side effects. CBC analysis revealed no difference between treatment groups in the concentrations of any circulating cell type (Total WBCs, neutrophils, lymphocytes, monocytes, eosinophils, basophils, platelets; Mann-Whitney U, n=7 mice/group). In blood collected from mice treated with GM-CSF, serum levels of the cytokine remained undetectable from 6 to 12 hours after intratumor injection (less than 14 pg/ml; 9 mice per group).

To evaluate the role of inflammation as a variable in the orthotopic injection model, we also injected palpable tumors in native PyMT+ mice with PBS or GM-CSF and compared tumor growth. GM-CSF similarly reduced tumor growth in PyMT+ murine breast cancers, while PBS injections did not (data not shown).

GM-CSF TREATMENT CORRELATES WITH REDUCED LUNG METASTASIS

PyMT breast cancers metastasize to the lung[30]. Because tumor angiogenesis is essential for metastases and GM-CSF stimulates macrophages to produce sVEGFR-1[19], we predicted that GM-CSF treatment reduced lung metastases. We orthotopically injected allograft tumors into FVB mice and treated them with GM-CSF or PBS. To enhance lung metastases, all tumors were allowed to grow to 2 cm in diameter before the mice were removed from the study. The lungs of these mice were insufflated, fixed whole, and stained with hematoxylin to identify tumor masses within the lungs (Figure 2A). GM-CSF treatment reduced the number of lung metastases compared to PBS (Figure 2B, $p=0.037$ by Mann-Whitney U, 6 mice per group).

GM-CSF LOWERS OXYGEN LEVELS WITHIN THE TUMOR PROPER

If reduction in tumor growth and metastasis in GM-CSF-treated mice resulted from sVEGFR-1 production and reduced angiogenesis, we predicted these mice would have reduced tumor oxygen levels. To track oxygen concentrations within the tumors of PBS- or GM-CSF-treated mice, we incubated an oxygen-sensitive nanoprobe (lithium octa-n-butoxy 2,3-naphthalocyanine [LiNc-BuO] microcrystals)[31] with PyMT tumor cells until the probe was internalized and injected these cells into the mammary fat pads of normal FVB female mice. High resolution, 3-dimensional EPR techniques analyzed oxygen tension within the tumors. GM-CSF-treated tumors demonstrated reduced oxygen levels compared to tumors treated with PBS (Figure 3, $p=0.050$ by repeated measures ANOVA). Distribution maps showed uniform probe allocation throughout the tumor, equal between groups, and limited in space to the tumor itself.

GM-CSF CAUSES INCREASED CELL DEATH WITHIN THE TUMOR AND CHANGES IN PATTERNS OF NECROSIS

Depriving tumors of oxygen and other nutrients causes cell death and tissue necrosis. To evaluate effects of oxygen deprivation on the tumors, we used fluorescent microscopy to assess the extent of cell death and necrosis in H&E-stained tumor sections[32]. Histological evaluation

showed GM-CSF-treated tumors had more tissue necrosis (reflected by enhanced fluorescence) compared to those treated with PBS (p=0.011 by Mann-Whitney U, Figure 4A). All tumors analyzed for necrosis were from mice with tumors of 2 cm diameter. Of particular note are the patterns of necrosis. Mice treated with PBS had focal patterns of necrosis with a single area of involvement near the tumor's outer surface. In contrast, GM-CSF-treated tumors revealed diffuse, multifocal patterns of necrosis, with smaller necrotic foci distributed throughout the tumor.

GM-CSF INCREASES MACROPHAGE, BUT NOT NEUTROPHIL NUMBERS IN TUMORS

Many different cell types compose murine breast tumors. To examine whether GM-CSF treatment altered the cell types infiltrating the tumor, we analyzed cell influx. We found increased F4/80+ (macrophage) staining within GM-CSF-treated tumors (p=0.014, Figure 4B), but found no differences in tumor neutrophils (7/4+ cells) (3.18% vs 4.49% 7/4+ cells, 7 and 9 mice per group, p=0.315 by Mann-Whitney U).

TUMOR-ASSOCIATED MACROPHAGES PRODUCE SVEGFR-1 IN RESPONSE TO GM-CSF TREATMENT

Since GM-CSF-treated macrophages produce and release sVEGFR-1[19], we hypothesized that GM-CSF induced TAMs to produce sVEGFR-1. We stained serial tumor sections for F4/80 expression and performed *in situ* hybridization for sVEGFR-1 mRNA expression. Grossly, GM-CSF- and vehicle-treated tumors looked different. Vehicle-treated tumors had uniform appearance, contrasting with irregular tissue variations seen in the GM-CSF-treated tumors. Not only did GM-CSF increase TAMs, but promoted inflammatory nodules, containing mostly F4/80+ macrophages. Macrophages in the GM-CSF-treated tumors produced sVEGFR-1 mRNA, especially along the interface between the nodules and the tumor cells (Figure 4C). PBS-treated tumors did not develop inflammatory nodules, or express high levels of sVEGFR-1 mRNA.

ADMINISTRATION OF GM-CSF CAUSES A SHIFT FROM M2 TO M1 POLARIZATION IN TUMOR-ASSOCIATED MACROPHAGES

Tumor-educated macrophages are usually M2 phenotype. To test effects of GM-CSF on macrophage polarization, we stained tumor sections for arginase I (M2 macrophages) and iNOS (M1 macrophages). Figure 4D shows that nearly all macrophages from PBS-treated tumors had an M2 phenotype (arginase I, green). In contrast, macrophages from GM-CSF-treated tumors exhibited M1 (iNOS, red) or transitional (double stain, yellow) phenotype macrophages. The highest concentrations of M1 macrophages were found near the inflammatory nodules that surrounded the necrotic tissues.

To assess whether GM-CSF administration elicited a shift in macrophage phenotype within the tumor environment, we extracted extracellular fluid (ECF) from snap-frozen tumor samples and measured the M2 cytokines IL-10 and IL-4. Both of these M2 cytokines were significantly lower in tumors treated with GM-CSF.

IDENTIFICATION OF SVEGFR-1 PRODUCING CELLS

To provide evidence that GM-CSF stimulated sVEGFR-1 expression in macrophages, we used flow cytometry to assess cells producing this factor. To distinguish between increased membrane-bound versus soluble VEGFR-1, we stained cells isolated from GM-CSF- or vehicle-treated tumors for both surface VEGFR-1 expression and total expression (including intracellular proteins). These studies (Figure 5) show that the relative numbers of CD68+ cells that express surface-bound VEGFR-1 did not change with GM-CSF treatment. Visual inspection of the plots suggests the emergence of a CD68+ population of cells that did not

express surface VEGFR-1. In contrast, treatment with GM-CSF caused a significant increase in a well-defined, $CD68^{HI}$ population of cells, all of which express VEGFR-1.

SVEGFR EXPRESSION MEDIATES THE EFFECTS OF GM-CSF TREATMENT

We suspected that reduced tumor growth rate was dependent on sVEGFR-1 activity. To test this hypothesis, we injected PyMT tumor cells into the mammary fat pad of normal FVB mice. Upon formation of a palpable tumor, the mice were randomized to one of the following four treatment groups: PBS, GM-CSF, GM-CSF plus a neutralizing antibody to sVEGFR-1, or GM-CSF plus an equimolar concentration of isotype IgG control antibody.

Treatment with a neutralizing antibody to sVEGFR-1 returned the growth rate of GM-CSF-treated tumors to near vehicle-treated levels (Figure 6A, p=0.006 overall, p=0.046 for GM-CSF + αsVEGFR vs GM-CSF + isotype by repeated measures ANOVA with Tukey post-hoc testing). In contrast, growth rates for GM-CSF-treated tumors and GM-CSF plus isotype-treated tumors were not different (p = 0.843). To ensure the results we observed were specific for physiologic alteration of the soluble VEGFR-1, and not confounded by binding of the antibody to the cell surface receptors, we also compared growth rates of tumors treated with PBS or anti-sVEGFR-1 alone. There were no differences between these groups (p=0.923, n=5 mice per group, data not shown).

GM-CSF TREATMENT REDUCES VESSEL DENSITY WITHIN THE TUMOR

According to our hypothesis, the lower oxygen levels observed in GM-CSF-treated tumors resulted from a sVEGFR-1-mediated block in angiogenesis. To test the effects of GM-CSF on blood vessel growth within the tumor, we injected mice with Texas Red-conjugated dextran (70 kD) five minutes prior to euthanasia. Tumors were removed, fixed, sectioned and analyzed by fluorescent microscopy. As shown in Figure 6B–C, GM-CSF treatment reduced the number of vessels in the tumor (p=0.023 by Kruskal-Wallis).

GM-CSF TREATMENT REDUCES DETECTABLE LEVELS OF VEGF IN THE TUMOR

Finally, when we extracted extracellular fluid from the tumors and subjected these samples to multiplex cytokine analysis for VEGF, we found a significant reduction in VEGF *detection* in the GM-CSF-treated tumors (Figure 6D, p=0.038). Since the ELISA antibody binds an epitope blocked by sVEGFR-1[19], this finding is consistent with reduced VEGF activity in the treated samples from the actions of sVEGFR-1.

DISCUSSION

This manuscript presents the novel observation that tumor-associated macrophages can be re-educated in murine breast cancer to an anti-angiogenic, anti-tumor growth and M1 phenotype by local treatment of the tumor with GM-CSF. Understanding the mechanisms of “tumor education” and basic macrophage biology allowed us to identify factors that alter macrophage behaviors within the tumor environment. Our data show that GM-CSF can re-educate TAMs to an anti-tumor phenotypes in a murine model of breast cancer through the production of sVEGFR-1.

GM-CSF treatment slowed tumor growth and prevented lung metastasis in our mouse model. This approach contrasts with previous work which focused on the strategy of limiting mononuclear phagocyte trafficking to the tumor to reduce tumor growth[15]. Our data show that reducing macrophage trafficking to murine breast cancers is not required for therapeutic benefit, but that re-educating the TAMs produced nearly identical effects. In our orthotopic studies, we find increased numbers of TAMs in tumors treated with GM-CSF, and still demonstrate improved outcomes. The effects of GM-CSF are robust, especially in light of the

aggressive nature of the PyMT tumor model[30]. To address the possibility of the orthotopic injection inducing a local inflammatory response that may have contributed to the anti-tumor effects of GM-CSF, we performed the same studies on PyMT+ transgenic mice. We treated a single mammary tumor with GM-CSF or PBS following the same schedule as our orthotopic allograft model and observed similar results (data not shown).

Because our model for lung metastases required both GM-CSF- and PBS-treated tumors to grow to the same size prior to sacrifice, lowered numbers of lung metastases suggest that GM-CSF impacted the tumor microenvironment (these PyMT tumors do not express GM-CSF receptors). We are actively investigating if GM-CSF treatment limited liberation of tumor cells from the primary tumor or had alternate effects on other factors like reducing tumor intravasation. These questions are being investigated in our laboratory.

In the orthotopic studies, we took advantage of *in vivo*, intratumor oxygen measurement by EPR as a surrogate for angiogenic activity. Most rapidly growing tumors have large oxygen demands. This demand must be met by the production of new blood vessels to deliver nutrients and oxygen. We found reduced oxygen levels within the tumors of GM-CSF-treated mice, correlating with reduced angiogenesis. This evidence supports the hypothesis that the production of sVEGFR-1 by TAMs blocks functional vessel development. The effects of treatment are especially noticeable in the 3D imaging, where effects at the border of the tumor can be separated from measurements within the tumor (e.g., tumors in GM-CSF-treated mice have less than 5 mmHg O_2 across ~90% of the tumor by 3D measures at week 3).

Altered amounts and patterns of necrosis found in GM-CSF-treated tumors illustrate the biological significance of oxygen deprivation, and provide outcomes which correlate with reduced angiogenesis and oxygen delivery to the tumors. Differing patterns of necrosis in GM-CSF- vs. vehicle-treated tumors correlate with macrophage distribution and behavior in the focal nodules of inflammatory cell accumulation throughout the tumor (see discussion of IHC and ISH below).

Reduced levels of functional angiogenesis at three weeks confirm that the mechanism behind the GM-CSF effect includes angiogenic blockade. Patterns of blood vessel growth in treated tumors appear more like normalized or physiologic vasculature[33], as opposed to the highly irregular, tortuous patterns of growth seen in untreated tumors or in mice treated with neutralizing antibodies to sVEGFR-1. These patterns correlate well with other studies examining the biological effects of VEGF blockade in patients treated with bevacizumab[34].

We propose that this anti-angiogenic activity is attributable to a change in TAM phenotype within the tumor, marked by the expression of sVEGFR-1. Until now, most tumors (especially those of the breast) show strong negative correlation between macrophage infiltration and outcome[6, 35, 36]. In the current studies, we reduced rates of breast cancer growth and metastasis *despite* increasing the number of macrophages in the GM-CSF-treated tumors. We conclude from this data that we have successfully reeducated the TAMs within these tumors—manipulating their behavior to affect desirable outcomes.

Macrophages in these areas also demonstrated a phenotype switch from M2 polarization, typically associated with tumor-associated macrophages to an anti-tumor, M1 phenotype. Cytokines responsible for driving macrophages toward the M2 phenotype, which is typically associated with tumor-associated macrophages, were also greatly reduced by GM-CSF treatment.

Neutralization of sVEGFR-1 with blocking antibodies shows definitive evidence that this important antiangiogenic factor largely mediates the effects of GM-CSF treatment on tumor growth. However, sVEGFR-1 blockade did not completely reverse the effects of GM-CSF

treatment. Plausible explanations for this include 1) that the blocking antibody had less than 100% activity or 2) that other mechanisms can account for part of the GM-CSF effect. Others have explored the use of autologous tumor cells engineered to produce GM-CSF to treat human cancers, especially melanoma[37]. Their studies show that GM-CSF can stimulate the differentiation and activity of dendritic cells, activating the adaptive immune response to the tumor. These T-cell responses could also occur in the present model. Such effects likely account for at least a portion of the response not due to sVEGFR-1.

Taken together, our data show that GM-CSF reprogrammed TAMs to slow tumor growth by starving the tumors of oxygen and nutrients via increasing levels of sVEGFR-1 within the tumor, preventing angiogenesis. Such models provide a powerful platform for studying the involvement of macrophages and other cells in the processes which comprise malignant transformation. Detailed studies of the changes invoked by treatment within each cell type and within the tumor organ will help us understand the contributions made by each of the players within this complex environment to the process of malignant transformation.

ACKNOWLEDGMENTS

This project was funded by the National Institutes of Health (NCI 1K99CA131552-01, RO1HL63800, RO1HL67176, and PO1HL70294-01) and the Department of Defense Congressionally Directed Medical Research Program (BCRP 2005 BC050083). We would like to thank Dr. Anna Bratasz for her help with the EPR imaging.

REFERENCES

1. Hanahan D, Weinberg RA. The hallmarks of cancer. Cell 2000;100:57–70. [PubMed: 10647931]
2. Watson NF, Ramage JM, Madjd Z, Spendlove I, Ellis IO, Scholefield JH, Durrant LG. Immunosurveillance is active in colorectal cancer as downregulation but not complete loss of MHC class I expression correlates with a poor prognosis. Int J Cancer 2006;118:6–10. [PubMed: 16003753]
3. Tsuruma T, Yagihashi A, Hirata K, Torigoe T, Araya J, Watanabe N, Sato N. Interleukin-10 reduces natural killer (NK) sensitivity of tumor cells by downregulating NK target structure expression. Cell Immunol 1999;198:103–110. [PubMed: 10648124]
4. Demirkesen C, Büyükpinarbaşili N, Ramazanoğlu R, Oğuz O, Mandel NM, Kaner G. The correlation of angiogenesis with metastasis in primary cutaneous melanoma: a comparative analysis of microvessel density, expression of vascular endothelial growth factor and basic fibroblastic growth factor. Pathology 2006;38:132–137. [PubMed: 16581653]
5. Oka H, Shiozaki H, Kobayashi K, Inoue M, Tahara H, Kobayashi T, Takatsuka Y, Matsuyoshi N, Hirano S, Takeichi M, et al. Expression of E-cadherin cell adhesion molecules in human breast cancer tissues and its relationship to metastasis. Cancer Res 1993;53:1696–1701. [PubMed: 8453644]
6. Pollard JW. Tumour-educated macrophages promote tumour progression and metastasis. Nat Rev Cancer 2004;4:71–78. [PubMed: 14708027]
7. Lotem J, Sachs L. Cytokine control of developmental programs in normal hematopoiesis and leukemia. Oncogene 2002;21:3284–3294. [PubMed: 12032770]
8. Pollard JW. Role of colony-stimulating factor-1 in reproduction and development. Mol Reprod Dev 1997;46:54–60. [PubMed: 8981364]
9. Tang R, Beuvon F, Ojeda M, Mosseri V, Pouillart P, Scholl S. M-CSF (monocyte colony stimulating factor) and M-CSF receptor expression by breast tumour cells: M-CSF mediated recruitment of tumour infiltrating monocytes? J Cell Biochem 1992;50:350–356. [PubMed: 1334964]
10. Hagemann T, Robinson SC, Schulz M, Trümper L, Balkwill FR, Binder C. Enhanced invasiveness of breast cancer cell lines upon co-cultivation with macrophages is due to TNF-alpha dependent up-regulation of matrix metalloproteases. Carcinogenesis 2004;25:1543–1549. [PubMed: 15044327]
11. Eubank TD, Galloway M, Montague CM, Waldman WJ, Marsh CB. M-CSF induces vascular endothelial growth factor production and angiogenic activity from human monocytes. J Immunol 2003 Sep 1;171:2637–2643. [PubMed: 12928417]

12. Sapi E. The role of CSF-1 in normal physiology of mammary gland and breast cancer: an update. Exp Biol Med (Maywood) 2004;229:1–11. [PubMed: 14709771]
13. Scholl SM, Lidereau R, de la Rochefordière A, Le-Nir CC, Mosseri V, Noguès C, Pouillart P, Stanley FR. Circulating levels of the macrophage colony stimulating factor CSF-1 in primary and metastatic breast cancer patients. A pilot study. Breast Cancer Res Treat 1996;39:275–283. [PubMed: 8877007]
14. Kacinski BM. CSF-1 and its receptor in ovarian, endometrial and breast cancer. Ann Med 1995;27:79–85. [PubMed: 7742005]
15. Lin EY, Nguyen AV, Russell RG, Pollard JW. Colony-stimulating factor 1 promotes progression of mammary tumors to malignancy. J Exp Med 2001;193:727–740. [PubMed: 11257139]
16. Wyckoff J, Wang W, Lin EY, Wang Y, Pixley F, Stanley ER, Graf T, Pollard JW, Segall J, Condeelis J. A paracrine loop between tumor cells and macrophages is required for tumor cell migration in mammary tumors. Cancer Res 2004;64:7022–7029. [PubMed: 15466195]
17. Lin EY, Li JF, Gnatovskiy L, Deng Y, Zhu L, Grzesik DA, Qian H, Xue XN, Pollard JW. Macrophages regulate the angiogenic switch in a mouse model of breast cancer. Cancer Res 2006;66:11238–11246. [PubMed: 17114237]
18. Armstrong CA, Botella R, Galloway TH, Murray N, Kramp JM, Song IS, Ansel JC. Antitumor effects of granulocyte-macrophage colony-stimulating factor production by melanoma cells. Cancer Res 1996;56:2191–2198. [PubMed: 8616871]
19. Eubank TD, Roberts R, Galloway M, Wang Y, Cohn DE, Marsh CB. GM-CSF induces expression of soluble VEGF receptor-1 from human monocytes and inhibits angiogenesis in mice. Immunity 2004;21:831–842. [PubMed: 15589171]
20. Gimbrone MA Jr, Aster RH, Cotran RS, Corkery J, Jandl JH, Folkman J. Preservation of vascular integrity in organs perfused in vitro with a platelet-rich medium. Nature 1969;222:33–36. [PubMed: 5775827]
21. Folkman J, Cole P, Zimmerman S. Tumor behavior in isolated perfused organs: in vitro growth and metastases of biopsy material in rabbit thyroid and canine intestinal segment. Ann Surg 1966;164:491–502. [PubMed: 5951515]
22. Bando H, Weich HA, Brokelmann M, Horiguchi S, Funata N, Ogawa T, Toi M. Association between intratumoral free and total VEGF, soluble VEGFR-1, VEGFR-2 and prognosis in breast cancer. Br J Cancer 2005;92:553–561. [PubMed: 15668703]
23. Toi M, Bando H, Ogawa T, Muta M, Hornig C, Weich HA. Significance of vascular endothelial growth factor (VEGF)/soluble VEGF receptor-1 relationship in breast cancer. Int J Cancer 2002;98:14–18. [PubMed: 11857378]
24. Yamaguchi T, Bando H, Mori T, Takahashi K, Matsumoto H, Yasutome M, Weich H, Toi M. Overexpression of soluble vascular endothelial growth factor receptor 1 in colorectal cancer: Association with progression and prognosis. Cancer Sci 2007;98:405–410. [PubMed: 17214745]
25. Lamszus K, Ulbricht U, Matschke J, Brockmann MA, Fillbrandt R, Westphal M. Levels of soluble vascular endothelial growth factor (VEGF) receptor 1 in astrocytic tumors and its relation to malignancy, vascularity, and VEGF-A. Clin Cancer Res 2003;9:1399–1405. [PubMed: 12684411]
26. Aref S, El Sherbiny M, Goda T, Fouda M, Al Askalany H, Abdalla D. Soluble VEGF/sFLt1 ratio is an independent predictor of AML patient out come. Hematology 2005;10:131–134. [PubMed: 16019458]
27. Bratasz A, Pandian RP, Deng Y, Petryakov S, Grecula JC, Gupta N, Kuppusamy P. In vivo imaging of changes in tumor oxygenation during growth and after treatment. Magn Reson Med 2007;57:950–959. [PubMed: 17457861]
28. Chiesa-Vottero AG, Malpica A, Deavers MT, Broaddus R, Nuovo GJ, Silva EG. Immunohistochemical overexpression of p16 and p53 in uterine serous carcinoma and ovarian high-grade serous carcinoma. Int J Gynecol Pathol 2007;26:328–333. [PubMed: 17581420]
29. Kendall RL, Thomas KA. Inhibition of vascular endothelial cell growth factor activity by an endogenously encoded soluble receptor. Proc Natl Acad Sci U S A 1993;90:10705–10709. [PubMed: 8248162]
30. Lin EY, Jones JG, Li P, Zhu L, Whitney KD, Muller WJ, Pollard JW. Progression to malignancy in the polyoma middle T oncoprotein mouse breast cancer model provides a reliable model for human diseases. Am J Pathol 2003;163:2113–2126. [PubMed: 14578209]

31. Pandian RP, Parinandi NL, Ilangovan G, Zweier JL, Kuppusamy P. Novel particulate spin probe for targeted determination of oxygen in cells and tissues. Free Radic Biol Med 2003;35:1138–1148. [PubMed: 14572616]
32. Shaked Y, Ciarrocchi A, Franco M, Lee CR, Man S, Cheung AM, Hicklin DJ, Chaplin D, Foster FS, Benezra R, Kerbel RS. Therapy-induced acute recruitment of circulating endothelial progenitor cells to tumors. Science 2006;313:1785–1787. [PubMed: 16990548]
33. Willett CG, Boucher Y, di Tomaso E, Duda DG, Munn LL, Tong RT, Chung DC, Sahani DV, Kalva SP, Kozin SV, Mino M, Cohen KS, Scadden DT, Hartford AC, Fischman AJ, Clark JW, Ryan DP, Zhu AX, Blaszkowsky LS, Chen HX, Shellito PC, Lauwers GY, Jain RK. Direct evidence that the VEGF-specific antibody bevacizumab has antivascular effects in human rectal cancer. Nat Med 2004;10:145–147. [PubMed: 14745444]
34. Willett CG, Boucher Y, Duda DG, di Tomaso E, Munn LL, Tong RT, Kozin SV, Petit L, Jain RK, Chung DC, Sahani DV, Kalva SP, Cohen KS, Scadden DT, Fischman AJ, Clark JW, Ryan DP, Zhu AX, Blaszkowsky LS, Shellito PC, Mino-Kenudson M, Lauwers GY. Surrogate markers for antiangiogenic therapy and dose-limiting toxicities for bevacizumab with radiation and chemotherapy: continued experience of a phase I trial in rectal cancer patients. J Clin Oncol 2005;23:8136–8139. [PubMed: 16258121]
35. Lin EY, Pollard JW. Macrophages: modulators of breast cancer progression. Novartis Found Symp 2004;256:158–168. [PubMed: 15027489]
36. Mantovani A, Bottazzi B, Colotta F, Sozzani S, Ruco L. The origin and function of tumor-associated macrophages. Immunol Today 1992;13:265–270. [PubMed: 1388654]
37. Soiffer R, Lynch T, Mihm M, Jung K, Rhuda C, Schmollinger JC, Hodi FS, Liebster L, Lam P, Mentzer S, Singer S, Tanabe KK, Cosimi AB, Duda R, Sober A, Bhan A, Daley J, Neuberg D, Parry G, Rokovich J, Richards L, Drayer J, Berns A, Clift S, Cohen LK, Mulligan RC, Dranoff G. Vaccination with irradiated autologous melanoma cells engineered to secrete human granulocyte-macrophage colony-stimulating factor generates potent antitumor immunity in patients with metastatic melanoma. Proc Natl Acad Sci U S A 1998;95:13141–13146. [PubMed: 9789055]

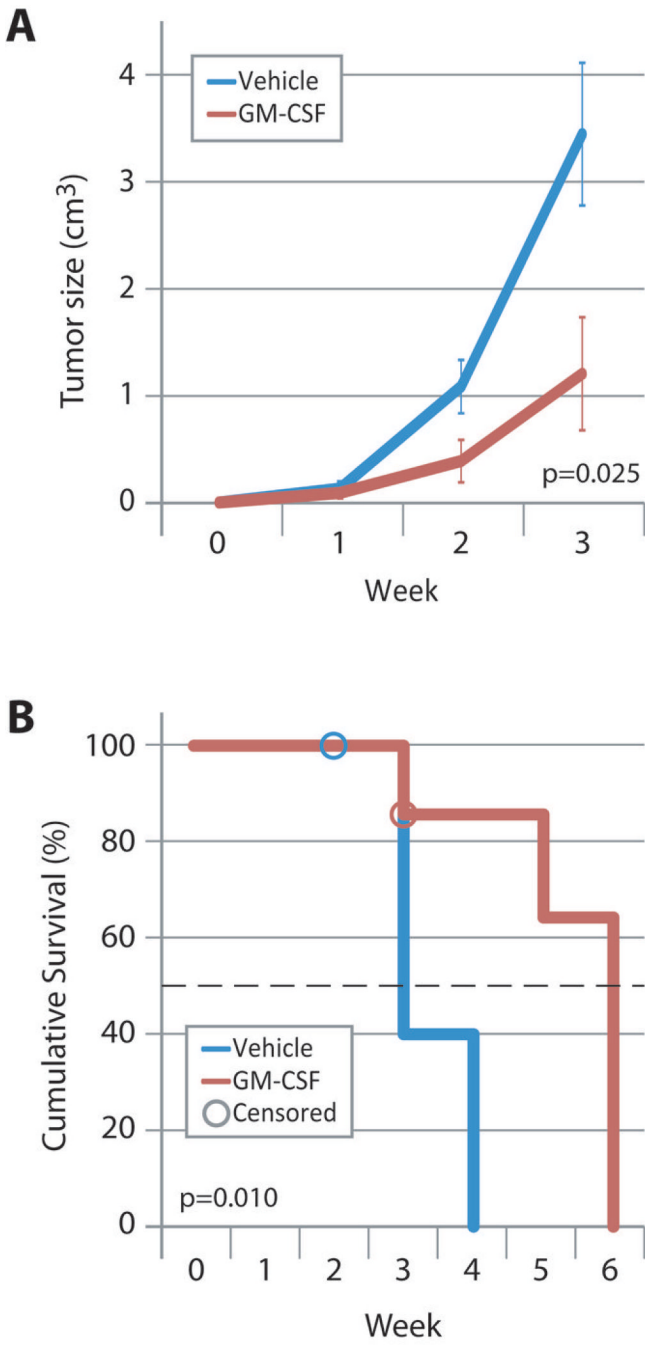

FIGURE 1. INTRATUMOR GM-CSF INJECTION SLOWS TUMOR GROWTH AND PROLONGS SURVIVAL

(A) FVB mice were injected with PyMT tumor cells into the left abdominal mammary fat pad. Upon palpable tumor formation, mice were treated with PBS or 100ng GM-CSF by intratumor injection three times per week until tumors reached the maximum size allowed by our ILACUC protocol. Data shown represent average tumor size ±SEM from eight (GM-CSF) and ten (PBS) mice. P=0.025 by repeated measures ANOVA.

(B) Kaplan-Meier analysis of mice shown in (A). Censored data (one mouse in each group) represent mice which died from causes other than tumor burden. Median survival was 3 weeks for vehicle-treated mice and 6 weeks for GM-CSF-treated mice. Survival in these studies is

defined as mice having tumors with a diameter <2 cm, which was criteria for euthanasia in the protocol approved by our IACUC. P=0.010 by Mantel-Cox nonparametric log rank test.

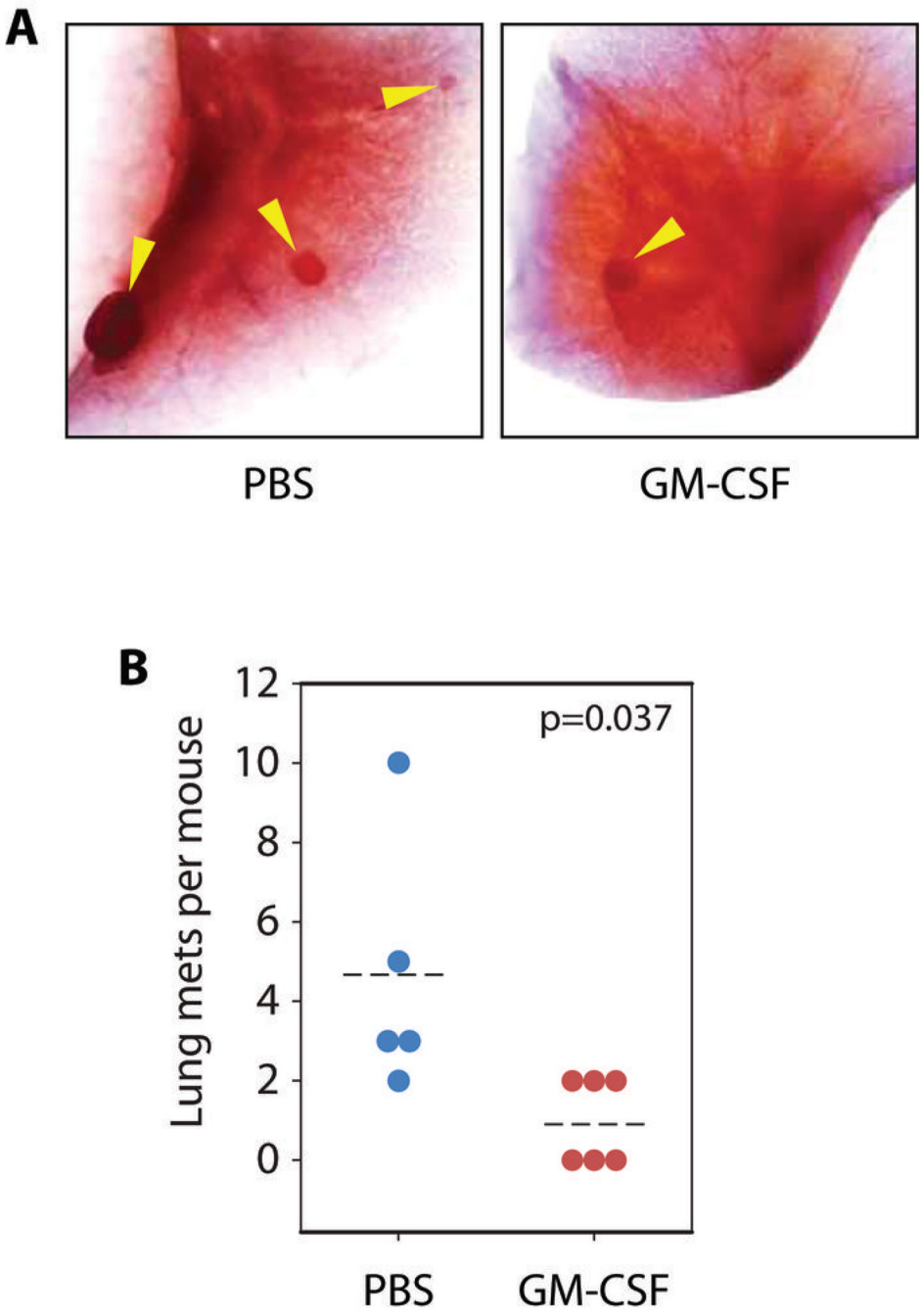

FIGURE 2. LOCAL GM-CSF TREATMENT REDUCES TUMOR METASTASES TO LUNG

(A) Representative images of lungs from GM-CSF and PBS-treated mice. Arrows show metastatic tumor growths, which appear as small opacities.

(B) Quantification of tumor metastases. Dotted line shows mean values over 5 mice (PBS) and 6 mice (GM-CSF) per group. P=0.037 by Mann-Whitney U test.

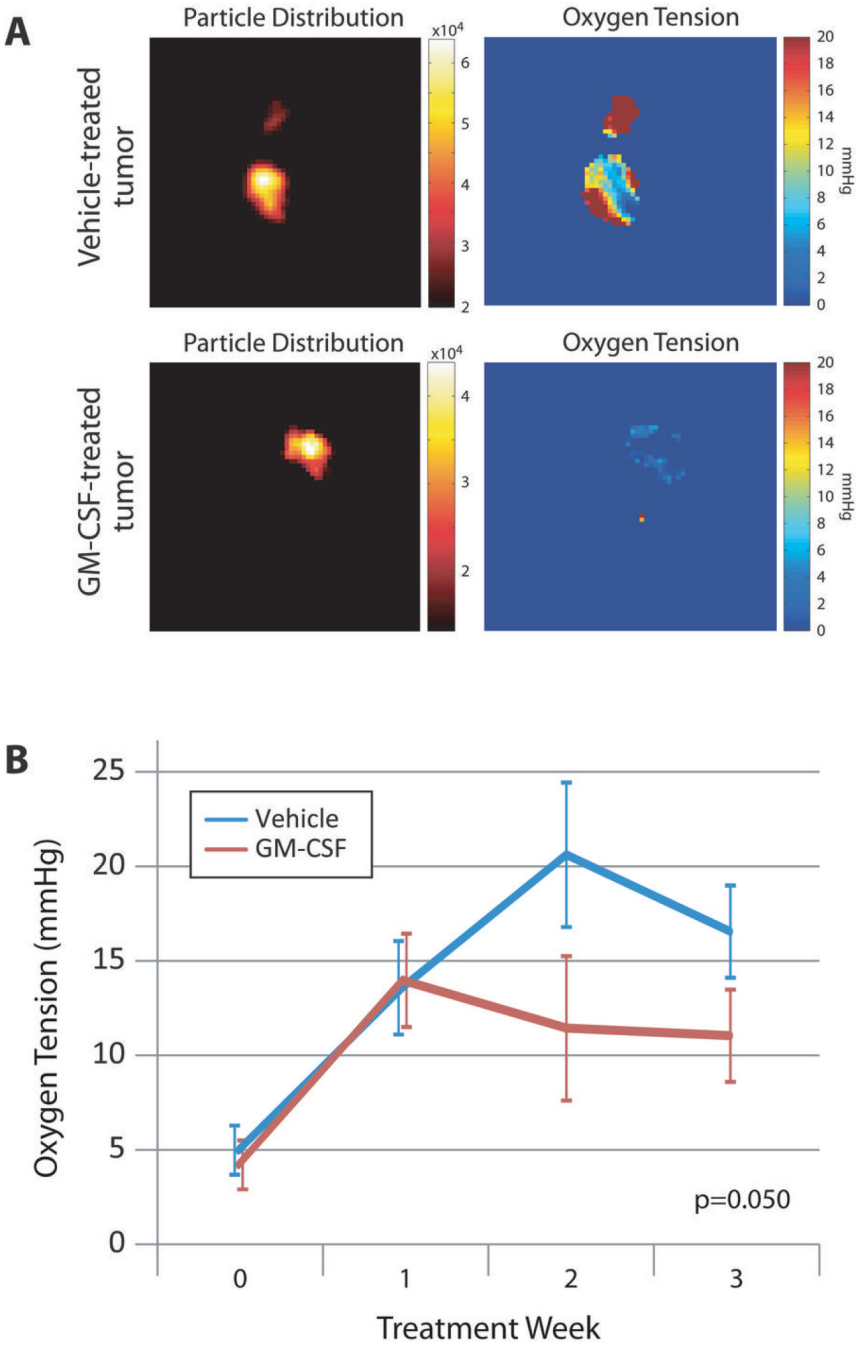

FIGURE 3. INTRATUMOR GM-CSF TREATMENT REDUCES OXYGEN LEVELS WITHIN MAMMARY TUMORS *IN VIVO*

(A) Representative samples of 3D EPR imaging showing particle distribution and oxygen tension throughout the tumor. Nanoparticles were uniformly distributed and limited in space to an area corresponding to the tumor proper. Numeric values on oxygen maps represent oxygen concentration in mmHg.

(B) Trends in tumor oxygen levels over time. Lines represent average oxygen concentration in mmHg taken from 2D EPR measurements ±SEM from 5 mice per group. P=0.050 by repeated measures ANOVA.

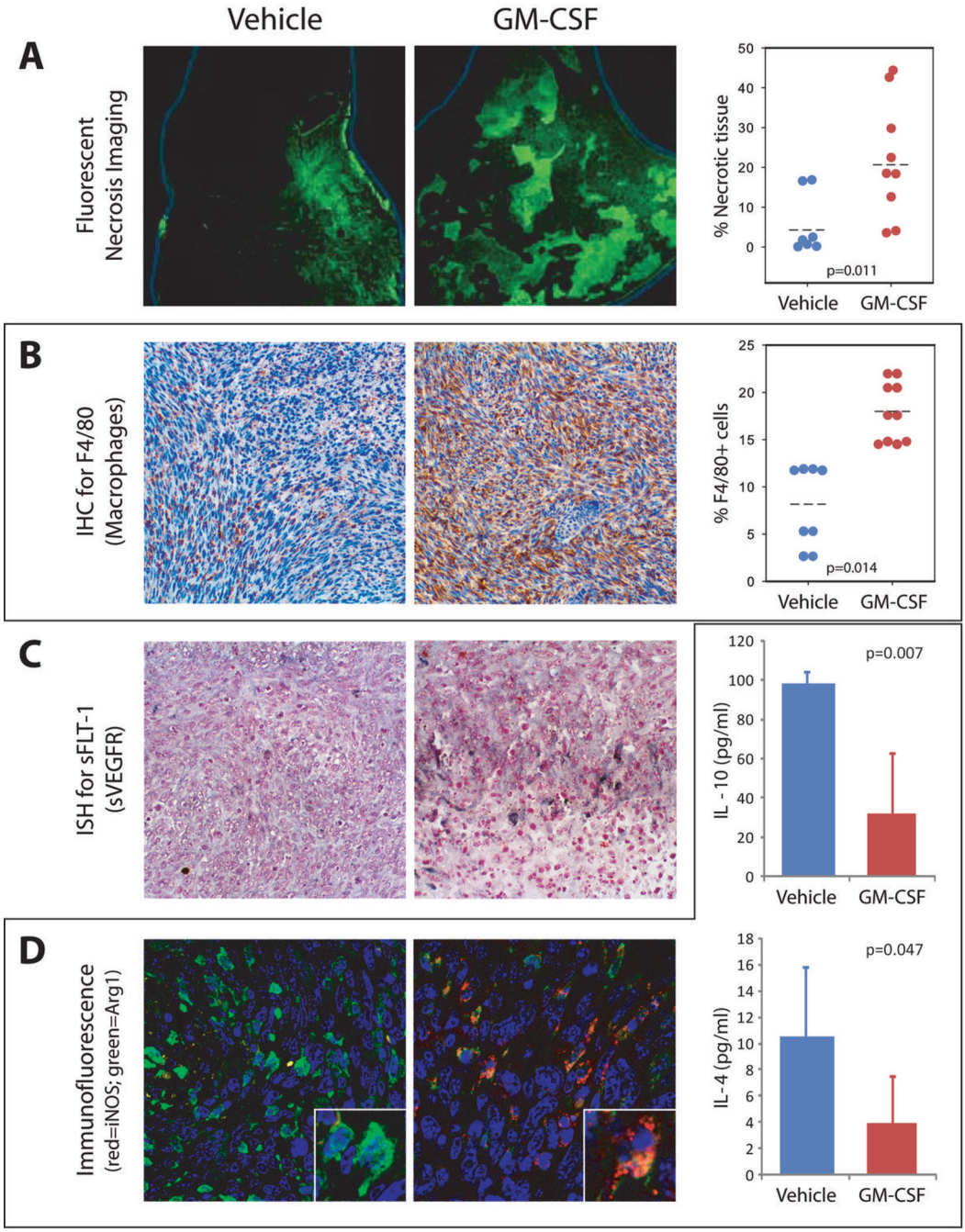

FIGURE 4. HISTOLOGICAL ANALYSIS OF TUMORS

(A) H&E sections were imaged at 10X under green fluorescence conditions. Under these conditions, necrotic tissue will autofluoresce allowing for identification of necrotic regions (*left and middle panels*). Necrotic regions were quantified (*right panel*) and compared to the area of the entire tumor section to obtain the percent necrotic tissue. P=0.011 by Mann-Whitney U.

(B) IHC for F4/80 (brown stain) shows number and distribution of macrophages in tumors treated with vehicle or GM-CSF (*left and middle panels*). GM-CSF-treated tumors contain accumulations of F4/80-positive cells around the necrotic areas. Macrophage numbers were digitally quantified by comparing the number of F4/80 positive pixels to the total number of

pixels in each high power field for stitched images taken across entire tumors (*right panel*). P=0.014 by Mann-Whitney U.

(C) ISH identified cells expressing mRNA for sVEGFR-1 (dark blue/black stained regions). sVEGFR-1-positive cell distribution and phenotype correlate well with macrophage phenotype and distribution, suggesting that these are the cells producing the sVEGFR-1.

(D) M1/M2 phenotyping assays. Immunofluorescence assays assessing M1 (iNOS, red) and M2 (arginase-1, green) macrophage polarity is shown on the left. Treatment with GM-CSF caused a shift in these same macrophages identified in (C) from an M2 phenotype (green) to transitional (yellow) and M1 (red) phenotypes. Extracellular fluid taken from 9 and 14 tumors per group was subjected to multiplex cytokine bead arrays for IL-4 and IL-10. The results shown in the graphs at the right indicate a significant decrease in tumor levels of these two cytokines that drive M2 differentiation. P=0.007 and 0.047 by independent samples T-test.

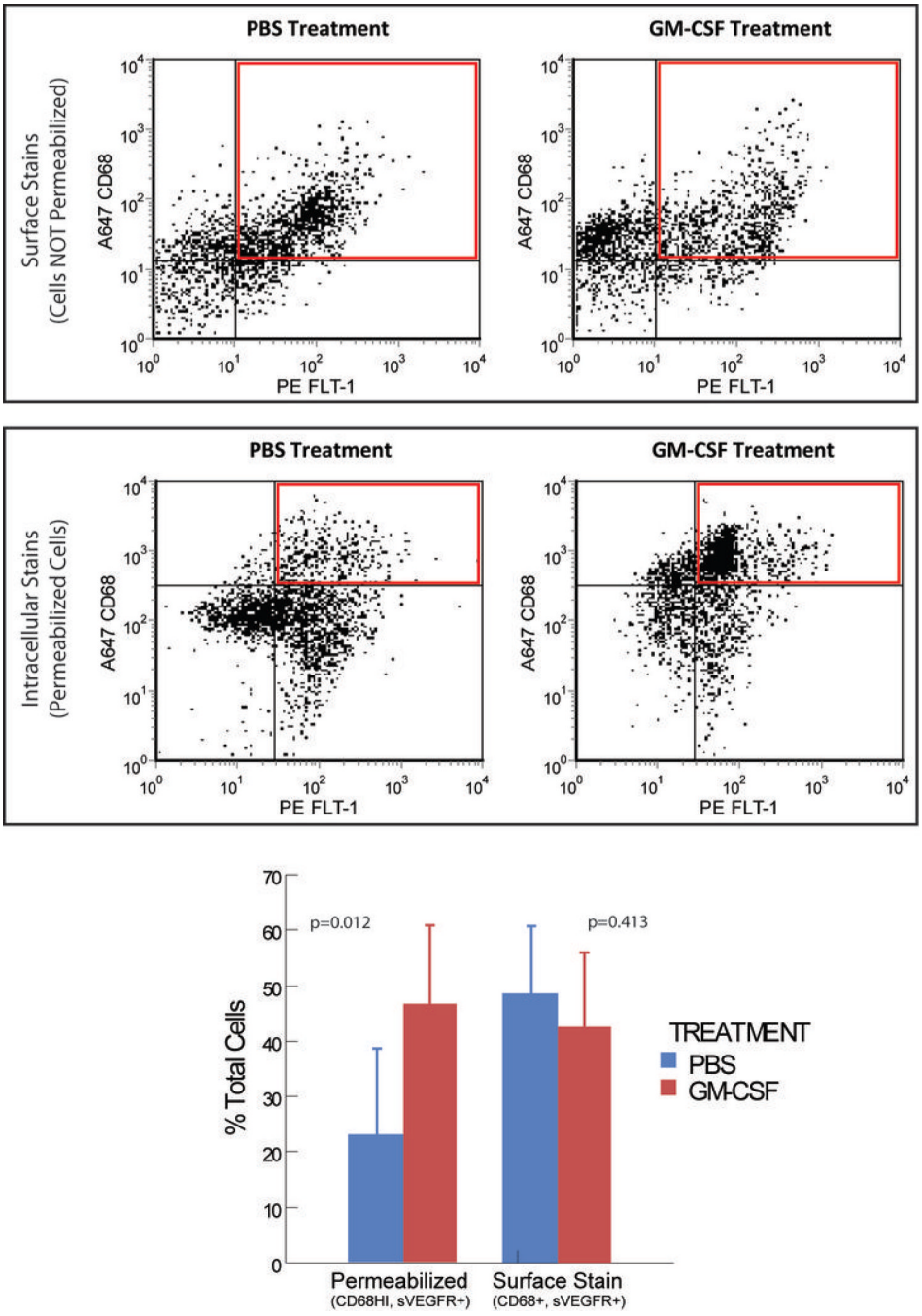

FIGURE 5. GM-CSF TREATMENT STIMULATES THE EMERGENCE OF A MACROPHAGE POPULATION THAT EXPRESSES VEGFR-1

Immune cells isolated from spontaneously-arising PyMT tumors that were treated with PBS or GM-CSF were stained with fluorescently-labeled antibodies targeting VEGFR-1 (FLT-1) and CD68, a macrophage marker. One set of cells (*top*) was stained for surface markers, while the other set (*bottom*) was permeabilized before staining, allowing analysis of intracellular proteins. The graph shows quantification of the relative abundance of cells represented by the red boxes shown on the graphs above. N=7 tumors per group (each mouse had one tumor injected with PBS and one with GM-CSF). P=0.012 and 0.413 by paired T tests, using mouse as the pairing variable.

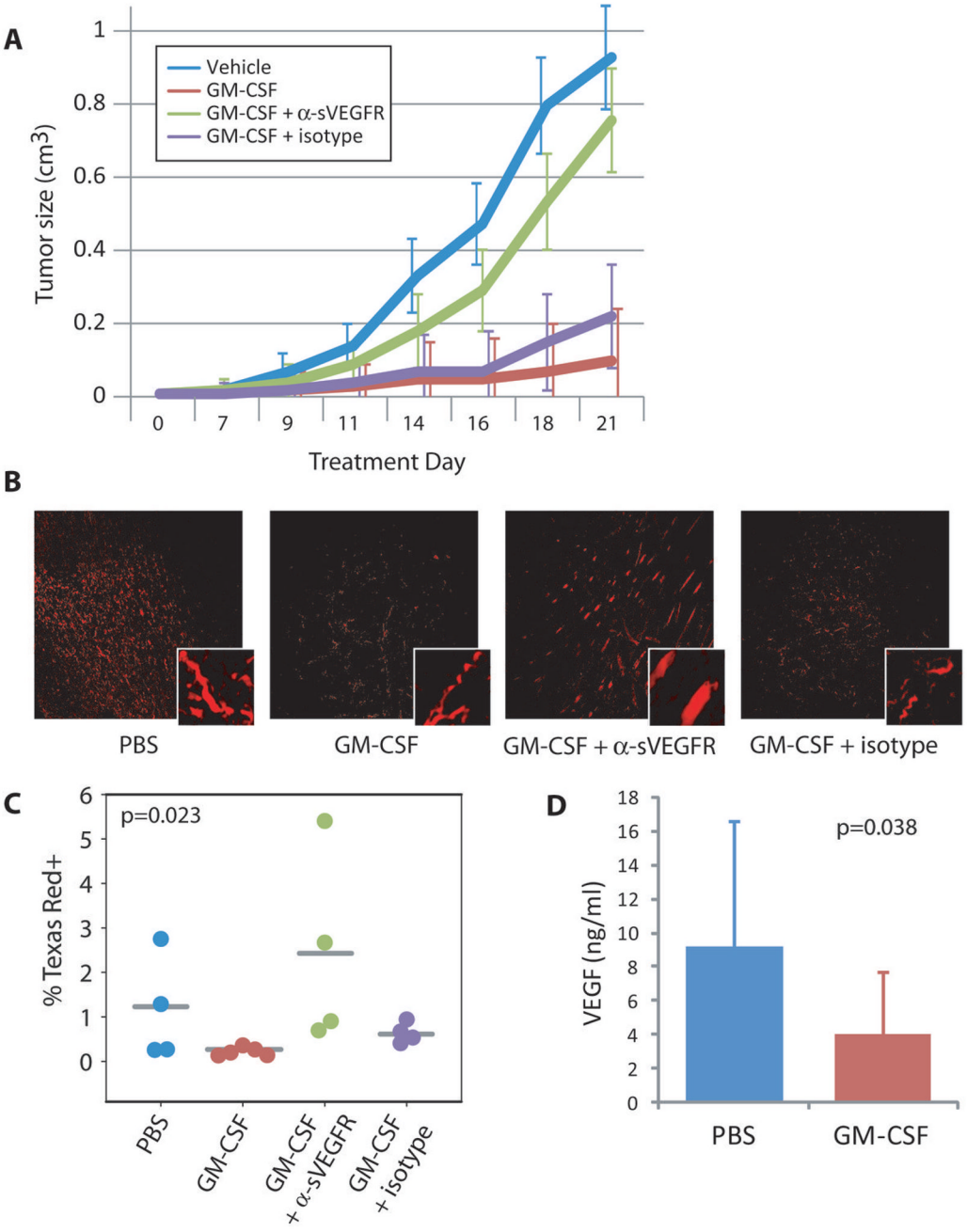

FIGURE 6. SVEGFR NEUTRALIZATION RESTORES NORMAL TUMOR GROWTH PATTERNS

(A) Graph shows change in tumor volume over time. Lines represent mean tumor size ± SEM for each group at each timepoint. Groups consisted of 4, 5, 8, and 4 mice, respectively. p=0.006 overall, p=0.046 for GM-CSF + αsVEGFR vs GM-CSF + isotype by repeated measures ANOVA with Tukey post-hoc testing.

(B) Mice were injected with a fluorescently-labeled dextran immediately before euthanasia. Harvested and sectioned tumors were then imaged with a fluorescent microscope to assess the extent of functional blood vessel development within the tumor.

(C) Representative samples from tumors taken from each group. Stitched images taken across the entire tumor section were digitally quantified for number of fluorescent pixels for each mouse. The average percent of Texas Red-positive pixels per mouse is shown in the graph. P=0.023 by Kruskal-Wallis test.
(D) Quantification of detectable VEGF levels in extracellular fluid (ECF). ECF was extracted from 9 PBS-treated and 14 GM-CSF-treated tumors and subjected to multiplex analysis for VEGF. VEGF detection is reduced when bound by sVEGFR-1. Average detected VEGF concentration is shown in the graph ± SD. P=0.038 by independent samples T test.